CHEMISTRY
A European Journal

A Journal of
ChemPubSoc Europe

Accepted Article

Title: Light-responsive Arylazopyrazole Gelators: From Organic to Aqueous Media and From Supramolecular to Dynamic Covalent Chemistry

Authors: Chih-Wei Chu, Lucas Stricker, Thomas Kirse, Matthias Hayduk, and Bart Jan Ravoo

To be cited as: *Chem. Eur. J.* 10.1002/chem.201806042

Link to VoR: http://dx.doi.org/10.1002/chem.201806042

Supported by
ACES

WILEY-VCH

10.1002/chem.201806042

WILEY-VCH

FULL PAPER

Light-responsive Arylazopyrazole Gelators: From Organic to Aqueous Media and From Supramolecular to Dynamic Covalent Chemistry

Chih-Wei Chu,‡ Lucas Stricker,‡ Thomas M. Kirse, Matthias Hayduk and Bart Jan Ravoo*[a]

Abstract: We report versatile photo-responsive gels based on tripodal low molecular weight gelators (LMWGs). A cyclohexane-1,3,5-tricarboxamide (CTA) core provides face-to-face hydrogen bonding and a planar conformation, inducing the self-assembly of supramolecular polymers. The CTA core was substituted with three arylazopyrazole (AAP) arms. AAP is a molecular photoswitch that isomerizes reversibly under alternating UV and green light irradiation. The *E*-isomer of AAP is planar, favoring the self-assembly, whereas the *Z*-isomer has a twisted structure, leading to a disassembly of the supramolecular polymers. Using tailor-made molecular design of the tripodal gelator, light-responsive organogels as well as hydrogels were obtained. Additionally, in case of the hydrogels, AAP was coupled to the core through hydrazones, so that the hydrogelator and hence the photo-responsive hydrogel could also be assembled and disassembled using dynamic covalent chemistry.

Introduction

Low molecular weight gelators (LMWGs) represent a viable alternative for the development of soft materials.[1–4] They can self-assemble via non-covalent interactions, such as hydrogen bonding,[5,6] host-guest (e.g. crown ether-cation),[7] metal-ligand,[8–11] and π-π interactions,[12,13] forming extended and entangled supramolecular polymers.[14–16] Depending on the solvents used in the gels, they can be classified as organogels (organic solvent) or hydrogels (aqueous media). Gelation of LMWGs typically occurs from the highest soluble state, e.g. high temperature and ionized form. Owing to the dynamic properties of LMWGs, their formation can be triggered by pH,[17,18] solvent,[19] temperature,[20] enzyme,[21,22] light[23,24] or addition of salt.[25,26] As a consequence, the solubility of the gelator is gradually reduced. Nucleation occurs and the growth of nanofibrils is initiated. Thus, self-assembly of LMWGs is most often a kinetic trapping process.[27,28] Recent applications of LMWGs include tissue engineering,[29,30] optoelectronic device, [31–33] sensors[34–36] and actuators.[37,38]

[a] C. -W. Chu, L. Stricker, T. M. Kirse, M. Hayduk and B. J. Ravoo
Organic Chemistry Institute and Center for Soft Nanoscience (SoN)
Westfälische Wilhelms-Universität Münster
Corrensstrasse 40, 48149 Münster, Germany
E-mail: b.j.ravoo@uni-muenster.de

Supporting information for this article is given via a link at the end of the document.

Materials stimulated by light are of particular interest, since light is a non-invasive stimulus. Also, light irradiation can spatially and temporally target a specific area or spot on a surface or inside a material.[39,40] Photo-responsive gelators have gained increasing attention in recent years.[41] LMWGs comprising coumarins,[42,43] spiropyrans,[44] stilbenes,[45,46] azobenzenes[47,48] and dithienylethenes[49,50] were reported. Among them, azobenzenes are without doubt the most investigated class of photoswitches. However, it is known that the photo-isomerization of azobenzenes results in an equilibrium, the photostationary state (PSS), which is typically around 80% in both directions *E* to *Z* and *Z* to *E*.[51] This phenomenon of incomplete photo-isomerization can be even worse in solid phase materials due to the reduced dynamics required for isomerization of the azobenzene.[52,53] To address this limitation, arylazopyrazoles (AAPs) were recently introduced as improved light-responsive molecular switches.[54–56] In further studies, we and others investigated the properties of AAPs[57] as molecular switches and developed several supramolecular systems ranging from colloidal host-guest complexes,[58,59] foams,[60] adhesives[61] and DNA complexes.[62,63] Recently, also a light-responsive peptide hydrogel featuring host-guest interactions between AAP peptides and cyclodextrin vesicles was introduced by our group.[64]

A particularly versatile class of supramolecular polymers assembles from tripodal “core-arm” small molecules. In most cases, these supramolecular polymers are based on cyclohexane[65,66] or benzene[67,68] cores. Benzene-1,3,5-tricarboxamide (BTA) derivatives established by Meijer and co-workers are distinguished examples of tripodal monomers with benzene as core and variable functionalities connected to the core by amide bonds.[68] The intermolecular hydrogen bonding provided by the amides initiates the self-assembly. By appending different arms to the BTA core, diverse soft materials and applications, including hydrogels,[69,70] protein recognition,[71,72] imaging[67] and catalysis[73] were developed. Similar to BTA, cyclohexane-1,3,5-tricarboxamide (CTA) also affords intermolecular face-to-face hydrogen bonding and in addition, displays conformational flexibility. The flexible cyclohexane core permits the optimal stacking of the LMWGs and forms an extended supramolecular polymer. More interestingly, if hydrazones are applied to connect the arms and the core, dynamic and catalytic controlled *in situ* formation of hydrogels can be performed.[74–76] Under this circumstance, a hydrazide core and aldehyde arms are combined.[77] A detailed study of acid-catalyzed dynamic covalent gels was investigated by van Esch, Eelkema and co-workers with negatively charged liposomes[78] and patterned sulfonic acid surfaces.[79] The introduction of

10.1002/chem.201806042

dynamic covalent bonds such as hydrazones can not only facilitate the synthesis, but also broaden the possible application of dynamic molecular systems and materials, by simply mixing hydrazide core and aldehyde arms with diverse functions.[80–83]

Zhou et al. reported photo-responsive organogels based on a CTA core and arms comprising azobenzene units.[65] In their study, the light-induced sol-gel transition and thermal stability of the organogelator were explored. However, a rheological study of the organogel was not reported. Also, the overlapping UV/vis absorption of *E*- and *Z*-azobenzene potentially limits the reversibility of the sol-gel transition. Very recently, Venkataramani and co-workers reported tripodal AAP derivatives comprising a BTA core and demonstrated light-controlled rewritable imaging in the solid state.[67] From these preceding studies, we conclude that the combination of a CTA core and AAP arms is highly promising to develop versatile light-responsive LMWGs for both organic solvents and aqueous solutions.

Herein, we report a family of light-responsive tripodal LMWGs, in which the molecular design was pursued by the core-arm approach. The general design and the functions of each molecular component are described in Scheme 1. First of all, the CTA core allows optimal stacking by intermolecular hydrogen bonding. Secondly, the AAP moieties in the arms stabilize the self-assembly via π-π interactions and provide photo-response. Thirdly, the functionalities at the end of the arms increase solubility in the desired solvent and potentially give rise to higher-ordered self-assembly, such as bundles, enhancing gelation. Finally, the connections between the core and the arms are designed to be either permanent (amide) or dynamic covalent (hydrazone). The dynamic covalent approach can not only facilitate the *in situ* synthesis of hydrogelator, but also be used as a chemical stimulus for gel formation and disassembly. Light-response, rheology and dynamic properties of tripodal AAP based LMWGs are explored in this article.

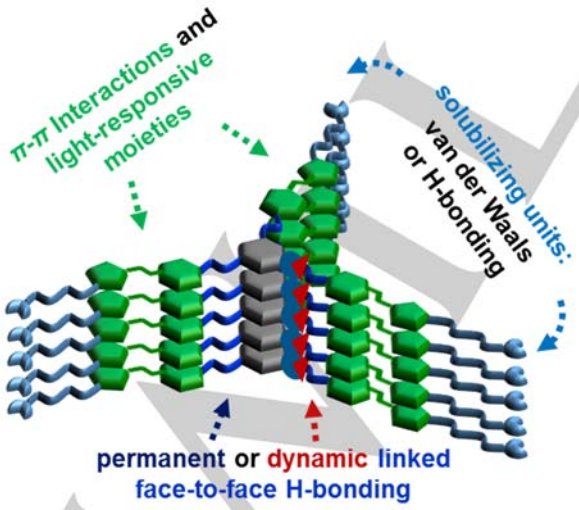

Scheme 1. Molecular design of tripodal cyclohexane-1,3,5-tricarboxamide (CTA) based gelators and the function of each molecular component to form supramolecular polymers and gels.

Results and Discussion

Molecular design and synthesis

A light-responsive organogelator (G1, Figure 1A) was synthesized using *cis*,*cis*-cyclohexane-1,3,5-tricarboxylic acid as a core allowing optimal stacking. An amine functionalized AAP was selected as arm. In addition, the AAP was equipped with a long alkyl chain at the end of each arm. This design offers excellent gelation properties by three kinds of interactions: (1) The amide link between core and arms forms hydrogen bonds and allows planar orientation of the AAP arms. (2) The AAP unit contributes π-π interactions of the aromatic rings and, more interestingly, provides light-responsive control of the stacking properties of the LMWG. (3) The aliphatic chain at the end of the arms creates an apolar exterior of the LMWG, yielding good solubility in organic solvents and additional dense packing by van der Waals interactions.

To enable biomimetic applications, hydrogels rather than organogels are desirable and hence the enhancement of water solubility is required. One straightforward approach is to maintain the molecular design of the organogelator G1, while attaching the amino acid alanine at the end of the arms (G2, Figure 1B). The terminal amino acid not only improves water solubility, but also presents additional hydrogen bonding between supramolecular polymers. Furthermore, using a closely similar molecular design, it was possible to introduce the dynamic covalent properties of hydrazones in the hydrogelator. For this purpose, a cyclohexanetrishydrazide (CTH) core and an aldehyde terminated AAP peptide (AAP-CHO) were prepared (Figure 1C). The hydrazone can be assembled by hydrazide and aldehyde under acidic (pH 4-6) or catalytic (e.g. aniline) conditions.[74] By exploiting the hydrolysis of glucono-δ-lactone (GdL) to generate acidic conditions, the hydrazone-linked hydrogelator (G3, Figure 1C) should potentially form *in situ*. Experimental details of the preparation of the precursors and gelators can be found in the supporting information.

Photo-isomerization of gelators

The photo-isomerization of gelators G1-G3 was investigated by UV/vis spectroscopy. It should be noted that the UV/vis

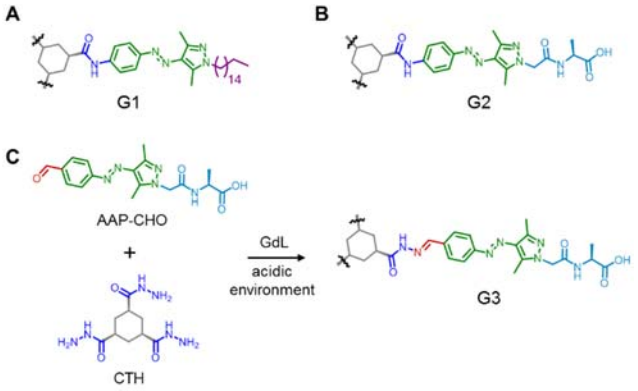

Figure 1. Molecular structure of amide-linked (A) organogelator (G1) and (B) hydrogelator (G2) and the *in situ* formation of (C) hydrazone-linked hydrogelator (G3) from CTH and AAP-CHO triggered by the hydrolysis of GdL.

10.1002/chem.201806042

measurements were carried out far below the critical gelation concentrations (see below). Thus, the spectrum of a solution of G1 (6.7 µM, as prepared) in toluene was measured (Figure 2A). Subsequently, the solution was irradiated with UV light (λ = 365 nm). Upon irradiation the typical changes in the absorbance spectra for the *E*-*Z* isomerization of AAPs could be observed.[54] The strong absorbance at 340 nm corresponding to the π-π* transition is reduced and blue-shifted, whereas the absorbance around 440 nm (n-π* transition) increases in intensity and shows a characteristic red-shift (Figure 2A). Upon irradiation with green light (λ = 520 nm), the original spectrum was observed with slightly higher intensity at 340 nm, indicating that in gelator G1 as prepared by chemical synthesis a small percentage of *Z*-isomer is present (Figure 2A). The photo-isomerization of G1 is reversible over at least four cycles without any sign of loss of efficiency (Figure 2B).

Quantification of the photoisomerization was carried out determining the PSS by NMR spectroscopy (Figure 2C). Due to the intermolecular stacking, G1 showed rather broad signals in the proton NMR. Therefore, a one-armed reference molecule G1-ref was used for NMR experiments. (Structure and analysis of G1-ref are provided in the supporting information). By integration of the proton signals in the aromatic region, the PSS for both the photo-isomerization from *E* to *Z* and from *Z* to *E* could be determined. It was found that in the solution of G1-ref as prepared the isomer ratio was 91:9 (*E*:*Z*), which changed drastically to 2:98 (*E*:*Z*) after irradiation with UV light (λ = 365 nm). After irradiation with green light (λ = 520 nm), the *E*-isomer was reobtained with 94:6 (*E*:*Z*). Again, this value is higher compared to the percentage of *E*-isomer in the initial spectrum, which is in a good agreement

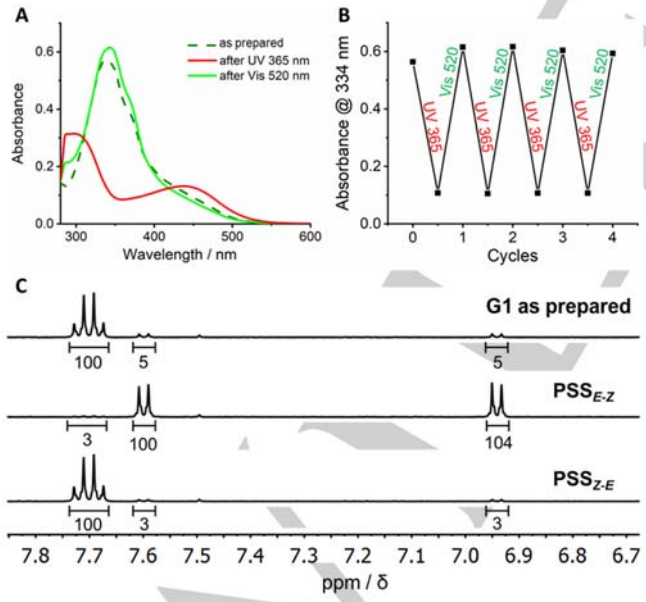

Figure 2. Photoisomerization of G1 confirmed by (A) UV/vis spectroscopy (6.7 µM in toluene). (B) Reversible *E*-*Z*-photoisomerization for four cycles. (C) Quantification of the *E*-*Z*-photoisomerization under UV and visible light irradiation. PSS measurements were carried out using G1-ref in THF-d_8 (500 µM).

to the results obtained by UV/vis spectroscopy. In summary, G1 showed excellent light-response identical to the AAP derivatives reported previously by our group.[54]

Similar characteristics were found for the hydrogelators via the same approach using a combination of UV/vis and NMR measurements. Both G2 and G3 exhibited typical AAP UV/vis-spectra and showed fully reversible photoswitchability for at least five cycles (Figure S1 and S2). Besides, PSS measurements confirmed the excellent photoisomerization efficiency of both hydrogelators. For G2, it showed PSS of 93% for *E* to *Z* and 94% for *Z* to *E* (Figure S3). In the case of hydrazone based gelator G3, cyclohexane monohydrazide (CMH) was applied instaed of CTH to give G3-ref to avoid broad signals due to stacking in D_2O. After mixing CMH and AAP-CHO in presence of GdL overnight, PSS of 90% for *E* to *Z* and 89% for *Z* to *E* were observed (Figure S4). The spectroscopic data and PSS of gelators G1-G3 are summarized in Table 1.

Table 1. Absorbance maxima (λ_{max}) and photostationary state PSS of gelators G1-G3.

	π-π* λmax (nm)		n-π* λmax (nm)			
	E isomer	*Z* isomer	*E* isomer	*Z* isomer	PSS$_{E-Z}$ (%)	PSS$_{Z-E}$ (%)
G1	336	303	427	437	98[a]	94[a]
G2	347	314	419	437	93[b]	94[b]
G3	346	321	421	434	90[c]	89[c]

[a] NMR using G1-ref in THF-d_8. [b] NMR in DMSO-d_6. [c] NMR using G3-ref in D_2O.

Photoresponsive organogels

Gelation tests for organogelator G1 were performed using a range of organic solvents and increasing concentrations of G1 to determine the critical gelation concentration (CGC) (Table 2). A heating-cooling sequence was applied to obtain homogenous organogels. In each case, a known amount of G1 was added to 1 mL of solvent and heated until it was fully dissolved. Afterwards, the solution was allowed to cool down to room temperature and the gel formation was checked by a reverse-vial test. If a solution was obtained, the amount of G1 was increased stepwise until a gel was achieved. The results displayed in Table 2 document the formation of a transparent orange organogel (G) in 9 out of 17 tested solvents with rather low CGC (< 1 wt%). In most other solvents, the gelator did not show any significant solubility at room temperature and precipitated (P). An exception to this is chloroform, in which even at rather high amount of G1 (20 mg/mL) a clear solution was obtained (S). The formation of a chloroform gel might be possible at higher concentration of G1 but was not further investigated in this study. Table 2 shows that G1 gelates rather non-polar and aprotic solvents with exception of *n*-alkanes.

10.1002/chem.201806042

Table 2. Solvent tests for gelation of G1 and CGC in each solvent (G: gel, P: precipitate, S: solution).

Solvent	State	CGC (mg/mL)	Solvent	State	CGC (mg/mL)
n-Decane	P	—	THF	G	14
n-Hexane	P	—	$CHCl_3$	S	—
1-Bromohexane	G	7	DCM	G	4
Cyclohexane	G	6	EtOAc	P	—
Me-cyclohexane	G	14	Acetone	P	—
Xylene	G	8	DMF	P	—
Toluene	G	8	DMSO	P	—
Bromobenzene	G	6	ACN	P	—
Dioxane	G	7			

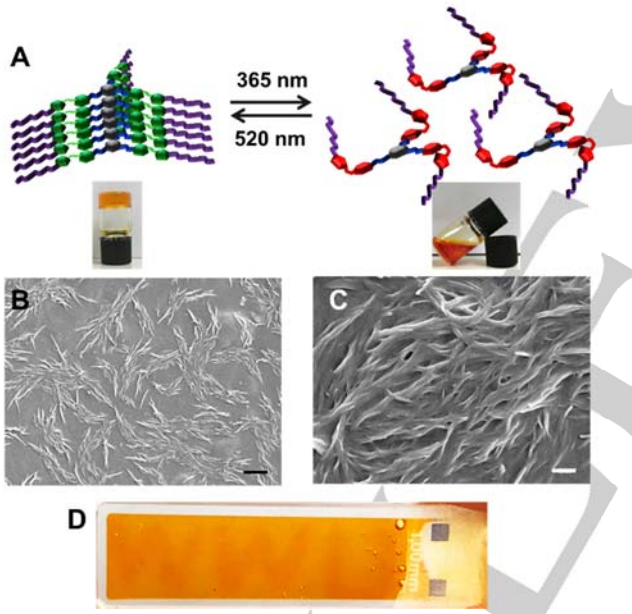

Figure 3. (A) Schematic representation of the sol-gel transition of G1 in under UV and green light irradiation in toluene. SEM images of 10 mg/mL G1 in toluene at (B) 5 k and (C) 25 k magnification (scale bars: (B) 2 µm and (C) 400 nm). (D) "WWU" was written in an organogel of 10 mg/mL G1 in toluene by UV light using a positive photomask.

No gelation is observed in polar solvents and solvents that can function as hydrogen bond donors.

Next, the light-response of the organogel were investigated in more detail. The organogels showed a distinct light-induced sol-gel transition (Figure 3A). For example, a heated solution of the planar *E*-isomer of G1 in toluene (10 mg/mL) forms an organogel upon heating then cooling due to intermolecular stacking of G1 as a result of hydrogen bonding, π-π- and van der Waals interactions. This gel fully liquefies upon irradiation with UV light due to the photo-isomerization of AAP from the planar *E*-isomer to the twisted *Z*-isomer.[53-55] The resulting twisted configuration of *Z*-G1 prevents intermolecular stacking, resulting in a clear solution. Upon green light irradiation, the planar *E*-isomer is re-obtained, the intermolecular interactions are restored, and an organogel is reformed that passes the reverse-vial test. As a control experiment a sample of the organogel was irradiated for 2.5 h with infrared light (980 nm), which does not induce isomerization of the AAP unit. As expected, in this experiment no gel-to-sol transition is observed. Thus, it can be concluded that the observed macroscopic changes are caused by the photo-isomerization of the AAP units and cannot be attributed to e.g. heating upon irradiation (Figure S10). The microstructures of the obtained gels were visualized by scanning electron microscopy (SEM) of a cast-dried organogel sample. In Figure 3B and 3C, it shows the formation of fibers in the scale of micrometers that entangle to a three-dimensional network typical for LMWG.

Upon close inspection of Figure 3A it can be observed that in comparison to the organogel of *E*-G1, the liquid state of *Z*-G1 has a more reddish orange color that is due to the increased and red-shifted absorbance of the n-π*-transition. Thus, the initials "WWU" of our university were written on the surface of the gel by UV irradiation through a positive photomask (Figure 3D). This observation indicates that these organogels can be applied for light-responsive patterning using a photomask, similar to what has been recently described by Venkataramani and co-workers for tripodal AAP derivatives in the solid state.[64]

Rheological measurements confirmed the viscoelasticity and the photo-response of the organogel prepared in toluene. Two different concentrations of the organogel, 10 and 15 mg/mL, were tested by frequency sweep measurements (Figure 4A). Both organogels displayed one order of magnitude higher storage modulus (G') than loss modulus (G"), indicating the formation of viscoelastic organogels that are fully stable for the entire frequency sweep. Also, a concentration dependency to the stiffness was observed, which a 15 mg/mL sample exhibited

10.1002/chem.201806042

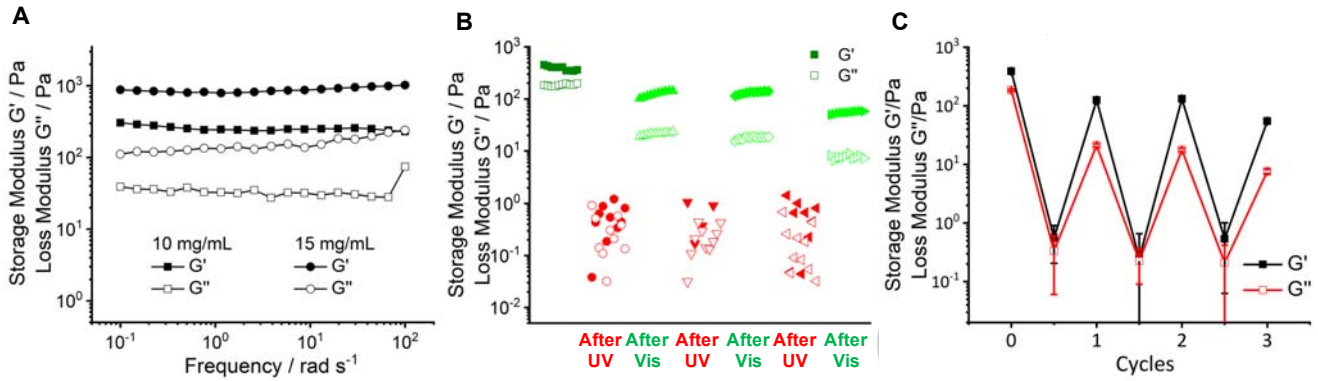

Figure 4. Rheological studies of G1 in toluene. (A) Frequency sweep for increasing gelator concentrations (10 and 15 mg/mL). (B) Oscillatory rheological measurements for light-responsive sol-gel transition of 15 mg/mL G1. (C) Reversible sol-gel transition for three cycles.

higher moduli, both G' and G", to the 10 mg/mL one. Then, the photo-response of the organogel was further investigated (Figure 4B). In the oscillatory rheological measurements, the original gel was first recorded. After irradiation with UV light for 5 min, another measurement was carried out. It showed a drastically reduced stiffness with almost three orders of magnitude. Moreover, randomly fluctuating points were observed for both moduli and even sometimes G" was over G', suggesting that a liquid-like material was obtained. As described above, we attribute this observation to disruption of intermolecular stacking by the twisted configuration of the *Z*-isomer of G1. After irradiation with green light for 5 min, over two orders of magnitude of G' was retrieved and again, stable moduli with G' over G" were observed. This observation is in accordance with the restoration of intermolecular stacking of the planar *E*-isomer of G1. Since the initial G' is retrieved, it can be excluded that the initial drop of G' can be attributed to mechanical disruption or heating of the gel during the rheological measurements. Two more irradiation cycles were carried out and a similar trend was observed, with high and stable moduli for the *E*-isomer and low and unstable moduli for the *Z*-isomer (Figure 4C).

Photoresponsive hydrogels

Since the formation of hydrogels from LMWGs is a kinetically controlled process, a smooth and homogeneous transition from the soluble and insoluble state of the gelator is critical. For peptide-based hydrogelators, tuning the pH is a popular and useful trigger to make hydrogels. In particular, making use of the slow hydrolysis of GdL to generate an acidic environment, a more homogenous hydrogel can be obtained.[84] Thus, G2 (2 or 5 mg/mL) was first dissolved in a "highly soluble state" (fully deprotonated at pH ~ 8). Upon the addition of GdL (5 or 10 mg/mL), the hydrogelator was gradually transferred into a "poorly soluble state" (partially protonated at pH ~ 5), since the apparent pK_a of alanine is around 5. Indeed, after standing in ambient conditions overnight, hydrogels were obtained that pass the reverse-vial test. Again, irradiation of this sample with infrared light (980 nm) does not lead to any softening of the hydrogel (Figure S10) The microstructure of the self-supporting hydrogels was confirmed by SEM (Figure S5).

The viscoelastic properties of the hydrogels were investigated by rheological measurements (Figure 5). Firstly, frequency-sweep oscillation experiments were performed. Similar to organogels of G1, almost one order of magnitude higher G' over G" were found for hydrogels of G2, indicating the success of hydrogel preparation. In general, the stiffness of the gel is proportional to both the gelator concentration and the amount of GdL. The higher the concentration of hydrogelator, the more and longer nanofibers are obtained. This leads to an increasingly cross-linked network and results in a stiffer gel. The amount of GdL determines the acidity of the gel solution. This is important for C-terminal peptide amphiphiles, since they show higher stiffness in more acidic

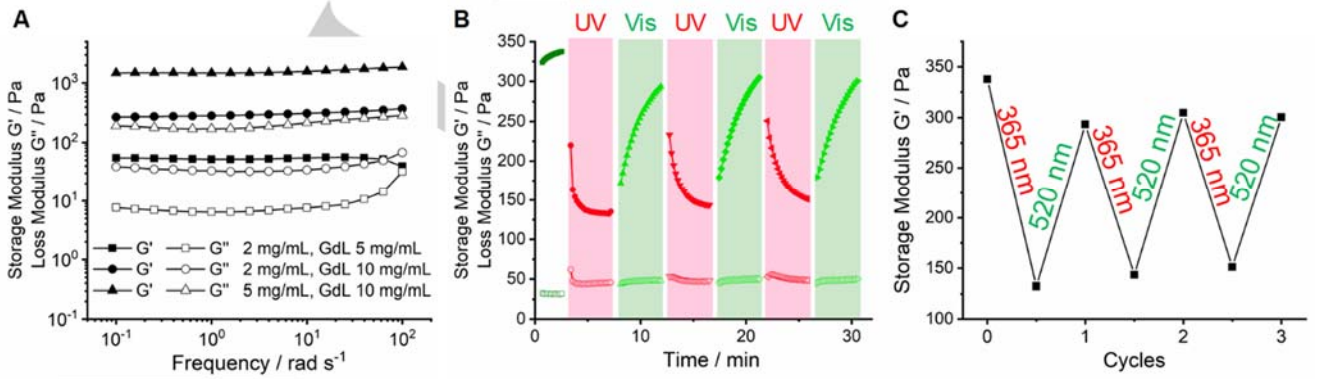

Figure 5. Rheological studies of G2. (A) Frequency sweep for increasing G2 and GdL concentrations. (B) Light-induced stiffness modulation under UV and visible light irradiation (2 mg/mL G2 and 10 mg/mL GdL). (C) Reversible storage modulus response to alternating UV and vis light irradiation for three cycles.

10.1002/chem.201806042

condition.[85] As shown in Figure 5A, the highest G' was found in 5 mg/mL G2 and 10 mg/mL GdL (solid triangles), while the lowest storage modulus was measured in the case of 2 mg/mL G2 and 5 mg/mL GdL (solid squares). By comparing the same hydrogelator concentration (2 mg/mL) with different amount of GdL, the hydrogel had almost 6-fold higher stiffness by increasing the GdL concentration from 5 mg/mL to 10 mg/mL. This observation is due to the higher degree of protonation of G2 obtained in a more concentrated GdL solution. Thus, more and longer nanofibers form, which make a stiffer hydrogel.

Next, the light-responsive modulation of stiffness for hydrogels prepared from G2 was examined (Figure 5B and C). The hydrogel formed with 2 mg/mL G2 and 10 mg/mL GdL was prepared one day before. The measurement started without any irradiation and the storage modulus showed a plateau value. Upon UV irradiation (λ = 365 nm), G' dropped by over 50% (Figure 5B). We attribute this to the photo-isomerization of the hydrogelator. Similar to G1, *E*-G2 is expected to provide a stiffer material due to the face-to-face hydrogen bonding and the π-π interactions between the gelators. On the contrary, the *Z*-G2 loses the additional π-π interactions between the AAPs due to their twisted structure.[53-55] Thus, a diminished elastic modulus (G') was observed. During the visible light irradiation (λ = 520 nm), the storage modulus was restored. This can be explained by the recovery of the planar structure of AAP in *E*-G2, which allows the restoration of π-π interactions (Figure 5B). Interestingly, during UV irradiation, the G' reached a plateau faster, whereas upon visible light irradiation, a plateau was reached rather slowly. A reasonable explanation for this observation is that upon UV irradiation, the hydrogel softens, and the oscillation enhances this process. In contrast, when the material stiffens during the green light irradiation, the oscillation disturbs the recovery of the fibers and the network. Nevertheless,

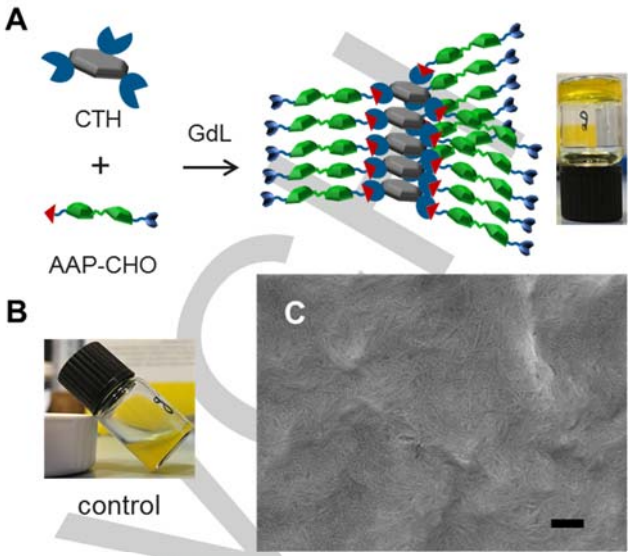

Figure 7. (A) *In situ* formation of G3 from CTH (2.5 mM) and AAP-CHO (15 mM) triggered by GdL (5 mg/mL). (B) Control experiment in absence of CTH (AAP-CHO: 15 mM and GdL: 5 mg/mL). (C) SEM image of 5 mM G3 (scale bar 200 nm).

the photo-isomerization of G2 induced a modulation of stiffness that can be repeated for at least three cycles (Figure 5C). It is noteworthy that during irradiation with either UV or green light the loss modulus remained almost constant. Additional photo-rheology experiments for different concentrations of samples (2 and 5 mg/mL G2 with 5 and 10 mg/mL GdL) can be found in the supporting information (Figure S6).

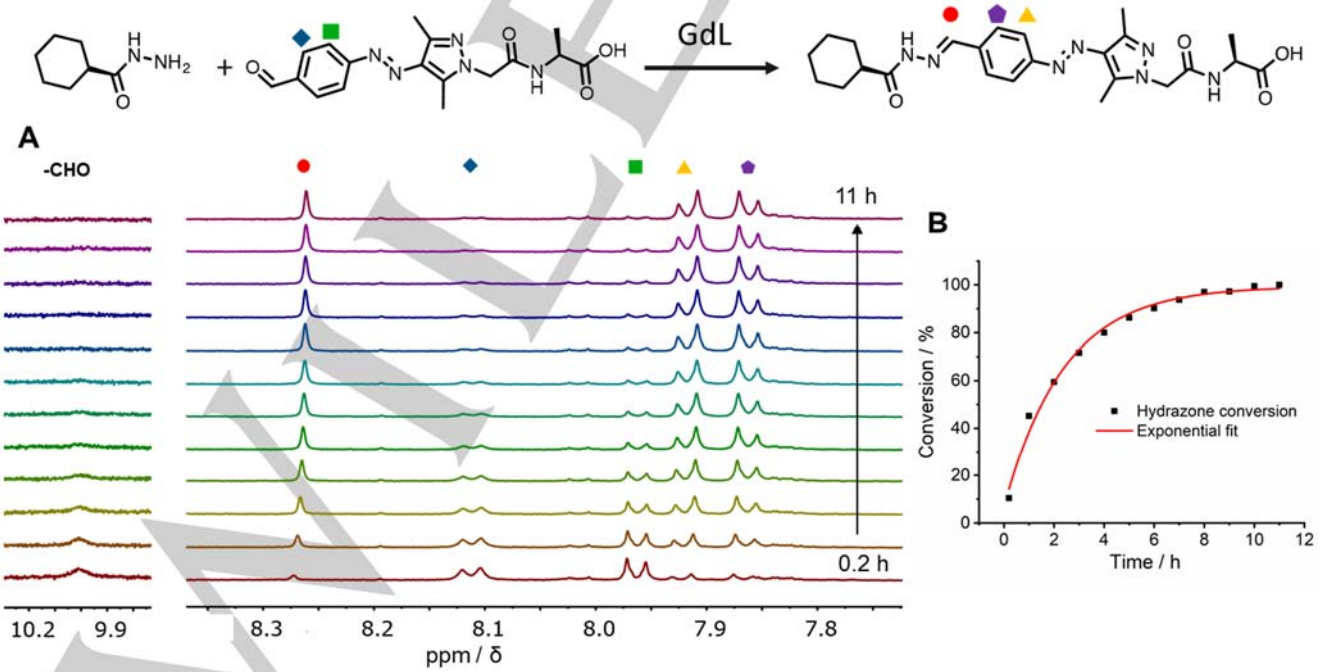

Figure 6. (A) GdL triggered formation of hydrazane G3-ref from CMH and AAP-CHO was carried out using proton NMR in D_2O (CMH: 500 μM, AAP-CHO: 500 μM and GdL: 1 mg/mL). (B) Formation of hydrazone in time based on the signal at 8.27 ppm.

10.1002/chem.201806042

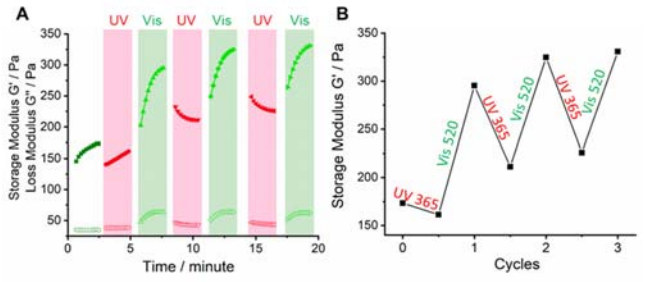

Figure 8. (A) Light-induced stiffness modulation of a hydrogel of 2.5 mM G3 triggered by 5 mg/mL GdL under UV and visible light. (B) Storage modulus response to light.

Photoresponsive and dynamic covalent hydrogels

Hydrogelator G3 containing dynamic covalent hydrazone bonds was synthesized *in situ* by employing GdL in the same fashion as describes above for G2, since the hydrazone formation is favored at pH 4-6, which is close to the apparent pK_a of alanine. To ensure that a tripodal gelator will form, excess arms to core (6:1) were employed in this study.[77] AAP-CHO (15 mM) and CTH (2.5 mM) were dissolved at pH ~ 8 and subsequently, GdL was added. After gentle mixing, the solution was left overnight. A self-supporting hydrogel was obtained and a schematic representation of the self-assembly is depicted in Figure 6A. Since the arms can be also considered as peptide amphiphiles (with AAP as hydrophobic tail and alanine as hydrophilic head group), a control experiment was carried out to ensure that the obtained hydrogels were achieved by the tripodal core-arm based hydrogelator G3. Indeed, when CTH was absent, a turbid solution with yellow precipitates of AAP-CHO was observed (Figure 6B). This finding supports our claim that the hydrogel is formed by the tripodal core-arm based hydrogelator G3. The self-assembled structures of the hydrogels were examined by SEM. Again, typical fibrous and cross-linked structures were found (Figure 6C).

To gain more information about the formation of G3, a kinetic study of the hydrazone formation was carried out. As a proof-of-principle, the formation of hydrazone between a hydrazide and an AAP-CHO in presence of GdL was tracked by proton NMR (Figure 7A). Similar to the determination of PSS for G1, in this study, a cyclohexane monohydrazide (CMH) was applied to avoid broadening proton signals due to intermolecular stacking of G3 in aqueous media. The decreasing signal of the aldehyde proton of AAP-CHO (at ~ 10 ppm) as well as the increasing signal of the hydrazone proton (red circle, 8.27 ppm) reveals the hydrazone formation. Besides, the large upfield shift of the ortho-protons at the benzyl ring of AAP supports our claim for the formation of a hydrazone. The more downfield shifted proton (blue rhombus, 8.12 ppm) is attributed to the presence of a strong electron withdrawing formyl group at the ortho position, instead, the more upfield shifted proton (purple pentagon, 7.86 ppm) is due to a more electron donating functional group, hydrazone. Integrating the hydrazone signal (red circle, 8.27 ppm) in 1 h intervals offers a quantitative measure of the hydrazone formation (Figure 7 and Figure S7). Experimental details are provided in the Experimental Section.

The viscoelastic properties of the hydrogels of G3 were also investigated by rheology. Similar to G2, frequency-sweep oscillation experiments were performed. Again, almost one order of magnitude higher G' over G" were found, indicating the success of hydrogel preparation. Again, the stiffness of the gel is proportional to both gelator concentration and the amount of GdL. The concentration of G3 refers to the concentration of CTH since an excess of AAP-CHO was applied. The highest G' was observed for 5 mM G3 with 10 mg/mL GdL and the lowest for 2.5 mM G3 with 5 mg/mL GdL (Figure S8). Then, oscillatory rheological measurements were performed to examine the light-response of the stiffness of G3. The hydrazone-linked hydrogel formed with 5 mM CTH, 30 mM AAP-CHO and 5 mg/mL GdL was prepared 24 h in advance. Similar to G1 and G2, *E*-G3 is expected to give a stiffer gel, whereas *Z*-G3 should give a softer gel. The measurements were carried out in the same fashion by recording firstly a non-irradiated sample and subsequently irradiating with UV and visible light in an alternating fashion for three cycles. Indeed, a light-responsive modulation of stiffness was observed similar to G2, i.e., higher G' for *E*-G3 and lower G' for *Z*-G3. The same explanation can be applied to these findings: planar configuration and additional π-π interactions for the *E*-isomer; twisted configuration and loss of π-π interactions for *Z*-isomer. After the first cycle, around 30% loss of storage modulus was found upon UV irradiation and in total three cycles of stiffness modulation were demonstrated (Figure 8A and B). We conclude that the introduction of amides (G2) or hydrazones (G3) to conjugate the core to the AAP arms does not significantly affect the formation of hydrogels nor their photo-response.

The formation of G3 involves a dynamic reaction between hydrazide core and aldehyde arms. This means that when other hydrazides (or aldehydes) are added, they can be used to tune the self-assembly of the gelator and the gel formation. Here, competitive experiments involving two different hydrazides were conducted. In the first assay, a neutral component, 4-hydroxylbutyric acid hydrazide was applied (Figure 9A). The addition of neutral hydrazide (NHy) suppresses the formation of G3 (prepared from 2.5 mM CTH, 15 mM AAP-CHO and 5 mg/mL GdL), since the probability for AAP-CHO to form a gelator (with CTH) or a non-gelator (with NHy) are equal. Thus, after one day, a self-supporting hydrogel was present in absence of the competitor, whereas a liquid remained in presence of NHy (5 or 25 mM). These findings are in agreement with our previous suggestions that the three-armed structure is required for the hydrogel formation. Interestingly, if the concentration of NHy is rather low (5 mM), a hydrogel is obtained after two days (Figure 9B). On the contrary, if the concentration of NHy is high enough (25 mM), the sample remains liquid-like even after five days (Figure 9C). This can be explained from the competing reactions of AAP-CHO with NHy and CTH and the consideration that the self-assembly of G3 is thermodynamically favoured. Only if sufficient three-armed gelator G3 is formed, the self-assembly will take place and as a result, a gel will form. When NHy is less concentrated, the formation of G3 is initially suppressed, but eventually wins out since the gel acts as a thermodynamic sink for G3. Also, a limited number of NHy arms will probably not disturb the self-assembly process. Instead, if NHy is more concentrated, the formation of G3 is suppressed to such an extent that no nucleation points for the formation of self-assembled nanofibrils are available, and no gelation occurs even after 5 days.

10.1002/chem.201806042

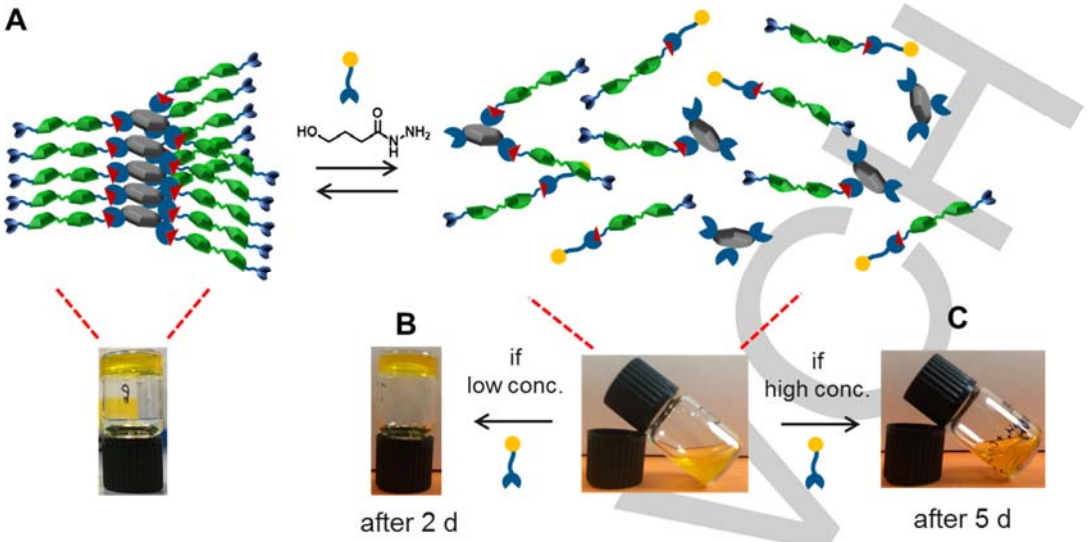

Figure 9. (A) Schematic representation of the dynamic properties of G3 in presence of a neutral hydrazide. Macroscopic pictures of G3 (2.5 mM CTH, 15 mM AAP-CHO and 5 mg/mL GdL) in presence of (B) 5 mM and (C) 25 mM of NHy.

In a final experiment, if a cationic hydrazide (CatHy, 5 mM), betaine hydrazide, was applied, gel formation was completely suppressed even at low concentration (Figure S9). This observation can be explained by considering the formation of cationic arms when CatHy reacts with CTH. The repulsion of the cationic arms disturbs the self-assembly of G3 and hence it persists in a liquid state.

Conclusions

In this study, we demonstrated that a family of light-responsive LMWGs can form gels in organic and aqueous media, and that the hydrogelator can have permanent (amide) or dynamic covalent (hydrazone) linkage. Tripodal LMWGs G1-G3, comprising a CTA core and three AAP arms, were successfully synthesized and fully characterized. The excellent photoisomerization efficiency of all gelators were confirmed by UV/vis and NMR spectroscopy. Organogelator G1 forms organogels in nine organic solvents with rather low CGC (< 1 wt%) and exhibits a reversible sol-gel transition under alternating UV and visible light irradiation. Homogeneous hydrogels prepared from G2 and G3 were obtained by tuning the pH through the hydrolysis of GdL. UV and visible irradiation was utilized to modulate the stiffness of the hydrogels. In both cases, the *E*-conformation of the hydrogelators represents the more stable and planar structure, which shows a higher storage modulus. On the contrary, the *Z*-isomer of both G2 and G3 disrupt the planarity and the additional π-π interactions contributed by AAPs, resulting in a lower storage modulus and a softer gel. Finally, the dynamic formation of G3 and its influence on the hydrogel properties was explored. Dynamically linked G3 was obtained *in situ* from a trihydrazide core (CTH) and AAP aldehyde arms (AAP-CHO). Neutral and cationic hydrazides were added to reverse the gel formation by hydrazone exchange. Our results demonstrate that molecular design of gelators with embedded photoswitches can lead to versatile light-responsive and dynamic soft materials. The stiffness of these materials can be modulated by light, which is especially important when considering biomedical applications such as tissue engineering.[86]

Experimental Section

Organogels. A certain amount of G1 was added to 1 mL of organic solvent and heated until it was fully dissolved. Afterwards, the solution was allowed to cool down to rt and the gel formation was checked by a reverse-vial test. If a solution was obtained, the amount of G1 was increased until a gel was achieved. The results displayed in Table 1 showed the formation of a transparent orange organogel (G) in 9 out of 17 tested organic solvents with different CGCs. Appearance of results was presented by gel (G), precipitate (P) and solution (S).

Hydrogels. Stock solutions of 10, 5 and 2 mg/mL of G2 were prepared in ddH_2O and NaOH (1 M) was used to adjust the pH until the hydrogelators were fully dissolved (pH ~ 9). In a glass vial containing 2, 5, 10, 20 mg/mL of GdL, 200 µL of different concentrations of the stock solution was added. After no crystals were observed, the solution was left overnight for gelation. Samples were defined as gels if a reverse vial test was passed. Critical gelation concentration was found in 2 mg/mL and the minimum required GdL was 5 mg/mL in this concentration.

Dynamic covalent hydrogels. Stock solutions of 5 and 10 mM of CTH and the correspondingly 30 and 60 mM of AAP-CHO were prepared. In a glass vial containing 2, 5, 10, 20 mg/mL of GdL, the core (CTH) and arm solutions (AAP-CHO) were mixed with a 1:1 fashion. After a clear solution was obtained, it was then left untouched for gelation overnight. Critical gelation concentration was found in presence of 2.5 mM of CTH and minimum required GdL was 5 mg/mL in this concentration.

Rheology and photoswitching experiments. Rheological measurements were performed by using a shear rheometer (MCR 102,

Modular Compact Rheometer, Anton-Paar) equipped with a glass plate (P-PTD200/GL) and CP25-2 cone plate (radius = 12.5 mm, cone angle = 2°, sample volume = 0.16 mL). The gap between two plates were fixed at 0.106 mm during the measurements. The measurement temperature was maintained at 20 °C. Frequency sweep measurements were carried out with a 0.2% strain amplitude. For irradiation experiments, the measurements were carried out with a 0.5% strain amplitude and 10 Hz frequency. The photoisomerization was induced by in situ irradiation from beneath the glass plate using LEDs as used in UV/vis spectroscopy. Photoswitching experiments were performed for three cycles.

Hydrazone formation. NMR spectroscopy was used to track the hydrazone formation between cyclohexane monohydrazide (CMH) and AAP-CHO triggered by GdL. Solutions of CMH and AAP-CHO in D_2O were prepared and mixed in a 1:1 fashion (final concentration: 500 µM). The above solution was then transferred to a vial containing 1 mg/mL GdL and well mixed before transferring to a NMR tube. NMR spectra were recorded every hour for in total 12 spectra.

Acknowledgements

We are grateful for the financial support from EC H2020 – Marie Skłodowska-Curie Actions – Innovative Training Network, Multi-App (project number: 642793) and the Deutsche Forschungsgemeinschaft (DFG EXC 1003). Lukas Ibing (MEET, WWU Münster) is acknowledged for SEM measurements.

Keywords: light-responsive materials • arylazopyrazole • dynamic covalent chemistry • supramolecular polymers • gels

[1] P. Terech, R. G. Weiss, *Chem. Rev.* **1997**, *97*, 3133–3160.
[2] L. A. Estroff, A. D. Hamilton, *Chem. Rev.* **2004**, *104*, 1201–1217.
[3] K. Tao, A. Levin, L. Adler-Abramovich, E. Gazit, K. Tao, *Chem. Soc. Rev.* **2016**, *45*, 3935–3953.
[4] S. Fleming, R. V Ulijn, *Chem. Soc. Rev.* **2014**, *43*, 8150–8177.
[5] S. Yagai, T. Nakajima, K. Kishikawa, S. Kohmoto, T. Karatsu, A. Kitamura, *J. Am. Chem. Soc.* **2005**, *127*, 11134–11139.
[6] S. Yagai, Y. Monma, N. Kawauchi, T. Karatsu, A. Kitamura, *Org. Lett.* **2007**, *9*, 1137–1140.
[7] X. Yan, D. Xu, X. Chi, J. Chen, S. Dong, X. Ding, Y. Yu, F. Huang, *Adv. Mater.* **2012**, *24*, 362–369.
[8] M. Enomoto, A. Kishimura, T. Aida, *J. Am. Chem. Soc.* **2001**, *123*, 5608–5609.
[9] N. Sreenivasachary, J.-M. Lehn, *Proc. Natl. Acad. Sci.* **2005**, *102*, 5938–5943.
[10] W. Weng, Z. Li, A. M. Jamieson, S. J. Rowan, *Macromolecules* **2009**, *42*, 236–246.
[11] M. M. Piepenbrock, G. O. Lloyd, N. Clarke, J. W. Steed, *Chem. Rev.* **2010**, *110*, 1960–2004.
[12] C. Rest, M. J. Mayoral, K. Fucke, J. Schellheimer, V. Stepanenko, G. Fernández, *Angew. Chem. Int. Ed.* **2014**, *53*, 700–705.
[13] S. S. Babu, V. K. Praveen, A. Ajayaghosh, *Chem. Rev.* **2014**, *114*, 1973–2129.
[14] L. Brunsveld, B. J. B. Folmer, E. W. Meijer, R. P. Sijbesma, *Chem. Rev.* **2001**, *101*, 4071–4098.
[15] T. Aida, E. W. Meijer, S. I. Stupp, *Science* **2012**, *335*, 813–817.
[16] Z. Yu, F. Tantakitti, T. Yu, L. C. Palmer, G. C. Schatz, S. I. Stupp, *Science* **2016**, *351*, 497–502.
[17] S. Grigoriou, E. K. Johnson, L. Chen, D. J. Adams, T. D. James, P. J. Cameron, *Soft Matter* **2012**, *8*, 6788–6791.
[18] H. Frisch, P. Besenius, *Macromol. Rapid Commun.* **2015**, *36*, 346–363.
[19] R. Orbach, L. Adler-Abramovich, S. Zigerson, I. Mironi-Harpaz, D. Seliktar, E. Gazit, *Biomacromolecules* **2009**, *10*, 2646–2651.
[20] S. Kiyonaka, K. Sugiyasu, S. Shinkai, I. Hamachi, *J. Am. Chem. Soc.* **2002**, *124*, 10954–10955.
[21] R. V. Ulijn, *J. Mater. Chem.* **2006**, *16*, 2217–2225.
[22] Z. Yang, G. Liang, B. Xu, *Acc. Chem. Res.* **2008**, *41*, 315–326.
[23] L. A. Haines, K. Rajagopal, B. Ozbas, D. A. Salick, D. J. Pochan, J. P. Schneider, *J. Am. Chem. Soc.* **2005**, *127*, 17025–17029.
[24] T. Muraoka, C. Y. Koh, H. Cui, S. I. Stupp, *Angew. Chem. Int. Ed.* **2009**, *48*, 5946–5949.
[25] L. Chen, G. Pont, K. Morris, G. Lotze, A. Squires, L. C. Serpell, D. J. Adams, *Chem. Commun.* **2011**, *47*, 12071–12073.
[26] A. Z. Cardoso, L. L. E. Mears, B. N. Cattoz, P. C. Griffiths, R. Schweins, D. J. Adams, *Soft Matter* **2016**, *12*, 3612–3621.
[27] J. Raeburn, A. Z. Cardoso, D. J. Adams, *Chem. Soc. Rev.* **2013**, *42*, 5143–5156.
[28] E. Mattia, S. Otto, *Nat. Nanotechnol.* **2015**, *10*, 111–119.
[29] D. M. Ryan, B. L. Nilsson, *Polym. Chem.* **2012**, *3*, 18–33.
[30] J. D. Hartgerink, E. Beniash, S. I. Stupp, *Science* **2001**, *294*, 1684–1688.
[31] M. Externbrink, S. Riebe, C. Schmuck, J. Voskuhl, *Soft Matter* **2018**, *14*, 6166–6170.
[32] D. A. Stone, A. S. Tayi, J. E. Goldberger, L. C. Palmer, S. I. Stupp, *Chem. Commun.* **2011**, *47*, 5702–5704.
[33] E. R. Draper, J. J. Walsh, T. O. McDonald, M. A. Zwijnenburg, P. J. Cameron, A. J. Cowan, D. J. Adams, *J. Mater. Chem. C* **2014**, *2*, 5570–5575.
[34] S. Kiyonaka, K. Sada, I. Yoshimura, S. Shinkai, N. Kato, I. Hamachi, *Nat. Mater.* **2004**, *3*, 58–64.
[35] Z. Qi, P. M. de Molina, W. Jiang, Q. Wang, K. Nowosinski, A. Schulz, M. Gradzielski, C. A. Schalley, *Chem. Sci.* **2012**, *3*, 2073–2082.
[36] Q. Lin, T.-T. Lu, X. Zhu, T.-B. Wei, H. Li, Y.-M. Zhang, *Chem. Sci.* **2016**, *7*, 5341–5346.
[37] A. Goujon, G. Mariani, T. Lang, E. Moulin, M. Rawiso, E. Buhler, N. Giuseppone, *J. Am. Chem. Soc.* **2017**, *139*, 4923–4928.
[38] J. Chen, F. K. C. Leung, M. C. A. Stuart, T. Kajitani, T. Fukushima, E. van der Giessen, B. L. Feringa, *Nat. Chem.* **2018**, *10*, 132–138.
[39] S. Yagai, A. Kitamura, *Chem. Soc. Rev.* **2008**, *37*, 1520–1529.
[40] S. Khetan, J. A. Burdick, *Soft Matter* **2011**, *7*, 830–838.
[41] E. R. Draper, D. J. Adams, *Chem. Commun.* **2016**, *52*, 8196–8206.
[42] E. R. Draper, T. O. McDonald, D. J. Adams, *Chem. Commun.* **2015**, *51*, 12827–12830.
[43] S. H. Kim, Y. Sun, J. A. Kaplan, M. W. Grinstaff, J. R. Parquette, *New J. Chem.* **2015**, *39*, 3225–3228.
[44] Z. Qiu, H. Yu, J. Li, Y. Wang, Y. Zhang, *Chem. Commun.* **2009**, 3342–3344.
[45] J. F. Xu, Y. Z. Chen, D. Wu, L. Z. Wu, C. H. Tung, Q. Z. Yang, *Angew. Chem. Int. Ed.* **2013**, *52*, 9738–9742.
[46] E. R. Draper, E. G. B. Eden, T. O. McDonald, D. J. Adams, *Nat. Chem.* **2015**, *7*, 848–852.
[47] J. K. Sahoo, S. K. M. Nalluri, N. Javid, H. Webb, R. V. Ulijn, *Chem. Commun.* **2014**, *50*, 5462–5464.
[48] K. Tiefenbacher, H. Dube, D. Ajami, J. Rebek, *Chem. Commun.* **2011**, *47*, 7341–7343.
[49] J. T. van Herpt, M. C. A. Stuart, W. R. Browne, B. L. Feringa, *Chem. Eur. J.* **2014**, *20*, 3077–3083.
[50] S. Wang, W. Shen, Y. Feng, H. Tian, *Chem. Commun.* **2006**, 1497–1499.
[51] S. K. M. Nalluri, J. Voskuhl, J. B. Bultema, E. J. Boekema, B. J. Ravoo, *Angew. Chem. Int. Ed.* **2011**, *50*, 9747–9751.
[52] R. Klajn, *Pure Appl. Chem.* **2010**, *82*, 2247–2279.
[53] S.-C. Cheng, K.-J. Chen, Y. Suzaki, Y. Tsuchido, T.-S. Kuo, K. Osakada, M. Horie, *J. Am. Chem. Soc.* **2018**, *140*, 90–93.
[54] L. Stricker, E.-C. Fritz, M. Peterlechner, N. L. Doltsinis, B. J. Ravoo, *J. Am. Chem. Soc.* **2016**, *138*, 4547–4554.
[55] C. E. Weston, R. D. Richardson, P. R. Haycock, A. J. P. White, M. J. Fuchter, *J. Am. Chem. Soc.* **2014**, *136*, 11878–11881.
[56] S. Crespi, N. A. Simeth, B. König, *Nat. Rev. Chem.* **2019**, DOI: 10.1038/s41570-019-0074-6.
[57] L. Stricker, M. Boeckmann, T. M. Kirse, N. L. Doltsinis, B. J. Ravoo, *Chem. Eur. J.* **2018**, *24*, 8639–8647.
[58] S. Engel, N. Möller, L. Stricker, M. Peterlechner, B. J. Ravoo, *Small* **2018**, *14*, 1704287.
[59] N. Möller, T. Hellwig, L. Stricker, S. Engel, C. Fallnich, B. J. Ravoo, *Chem. Commun.* **2017**, *53*, 240–243.
[60] M. Schnurbus, L. Stricker, B. J. Ravoo, B. Braunschweig, *Langmuir* **2018**, *34*, 6028–6035.
[61] S. Lamping, L. Stricker, B. J. Ravoo, *Polym. Chem.* **2019**, *10*, 638–690.
[62] J. Moratz, L. Stricker, S. Engel, B. J. Ravoo, *Macromol. Rapid Commun.* **2018**, *39*, 1700256.
[63] V. Adam, D. K. Prusty, M. Centola, M. Skugor, J. S. Hannam, J. Valero, B. Kloeckner, M. Famulok, *Chem. Eur. J.* **2018**, *24*, 1062–1066.
[64] C.-W. Chu, B. J. Ravoo, *Chem. Commun.* **2017**, *53*, 12450–12453.
[65] Y. Zhou, M. Xu, J. Wu, T. Yi, J. Han, S. Xiao, F. Li, C. Huang, *J. Phys. Org. Chem.* **2008**, *21*, 338–343.
[66] A. Brizard, M. Stuart, K. van Bommel, A. Friggeri, M. de Jong, J. van Esch, *Angew. Chem. Int. Ed.* **2008**, *47*, 2063–2066.

[67] S. Devi, A. K. Gaur, D. Gupta, M. Saraswat, S. Venkataramani, *ChemPhotoChem* **2018**, *2*, 806–810.
[68] C. Kulkarni, E. W. Meijer, A. R. A. Palmans, *Acc. Chem. Res.* **2017**, *50*, 1928–1936.
[69] D. Spitzer, V. Marichez, G. J. M. Formon, P. Besenius, T. M. Hermans, *Angew. Chem. Int. Ed.* **2018**, *57*, 11349–11353.
[70] S. Seibt, S. With, A. Bernet, H. Schmidt, *Langmuir* **2018**, *34*, 5535–5544.
[71] M. Á. Alemán García, E. Magdalena Estirado, L.-G. Milroy, L. Brunsveld, *Angew. Chem. Int. Ed.* **2018**, *57*, 4976–4980.
[72] M. K. Müller, L. Brunsveld, *Angew. Chem. Int. Ed.* **2009**, *48*, 2921–2924.
[73] L. N. Neumann, M. B. Baker, C. M. A. Leenders, I. K. Voets, R. P. M. Lafleur, A. R. A. Palmans, E. W. Meijer, *Org. Biomol. Chem.* **2015**, *13*, 7711–7719.
[74] J. Boekhoven, J. M. Poolman, C. Maity, F. Li, L. van der Mee, C. B. Minkenberg, E. Mendes, J. H. van Esch, R. Eelkema, *Nat. Chem.* **2013**, *5*, 433–437.
[75] Y. Zhou, Y. Chen, P. Zhu, W. Si, J. Hou, Y. Liu, *Chem. Commun.* **2017**, *53*, 3681–3684.
[76] F. Trausel, F. Versluis, C. Maity, J. M. Poolman, M. Lovrak, J. H. van Esch, R. Eelkema, *Acc. Chem. Res.* **2016**, *49*, 1440–1447.
[77] J. M. Poolman, J. Boekhoven, A. Besselink, A. G. L. Olive, J. H. van Esch, R. Eelkema, *Nat. Protoc.* **2014**, *9*, 977–988.
[78] F. Versluis, D. M. van Elsland, S. Mytnyk, D. L. Perrier, F. Trausel, J. M. Poolman, C. Maity, V. A. A. Le Sage, S. I. van Kasteren, J. H. van Esch, R. Eelkema, *J. Am. Chem. Soc.* **2016**, *138*, 8670–8673.
[79] A. G. L. Olive, N. H. Abdullah, I. Ziemecka, E. Mendes, R. Eelkema, J. H. van Esch, *Angew. Chem. Int. Ed.* **2014**, *53*, 4132–4136.
[80] J. M. Poolman, C. Maity, J. Boekhoven, L. van der Mee, V. A. A. le Sage, G. J. M. Groenewold, S. I. van Kasteren, F. Versluis, J. H. van Esch, R. Eelkema, *J. Mater. Chem. B.* **2016**, *4*, 852–858.
[81] S. J. Rowan, S. J. Cantrill, G. R. L. Cousins, J. K. M. Sanders, J. F. Stoddart, *Angew. Chem. Int. Ed.* **2002**, *41*, 898–952.
[82] R. J. Wojtecki, M. A. Meador, S. J. Rowan, *Nat. Mater.* **2011**, *10*, 14–27.
[83] P. Chakma, D. Konkolewicz, *Angew. Chem. Int. Ed.* **2019**, DOI 10.1002/anie.201813525.
[84] D. J. Adams, M. F. Butler, W. J. Frith, M. Kirkland, L. Mullen, P. Sanderson, *Soft Matter* **2009**, *5*, 1856–1862.
[85] C. Tang, A. M. Smith, R. F. Collins, R. V. Ulijn, A. Saiani, *Langmuir* **2009**, *25*, 9447–9453.
[86] D. Seliktar, *Science* **2012**, *336*, 1124–1129.

10.1002/chem.201806042

WILEY-VCH

FULL PAPER

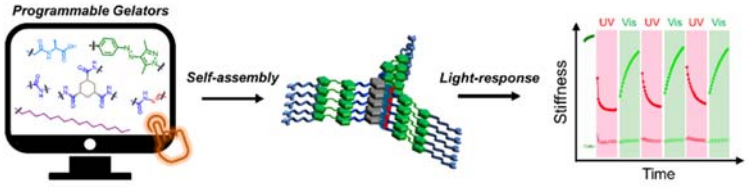

Programmable gelators: Tripodal core-arm gelators can be tailor-made by covalent and dynamic covalent linkages to form organo- and hydrogels. By incorporating arylazopyrazole as photoswiches, the stiffness of the gels can be modulated by light.

*Chih-Wei Chu,[‡] Lucas Stricker,[‡] Thomas M. Kirse, Matthias Hayduk and Bart Jan Ravoo**

Page No. – Page No.

Light-responsive Arylazopyrazole Gelators: From Organic to Aqueous Media and From Supramolecular to Dynamic Covalent Chemistry